



Instruments optimizations for low energy Gamma-ray detection

A. Morselli and G. Rodriguez

INFN Roma Tor Vergata, Via della Ricerca Scientifica, 1, 00131 Roma, Italy
e-mail: aldo.morselli@roma2.infn.it

Abstract. There is an experimental gap in the study of the non-thermal universe in the photon energy range from 300 keV to 5000 keV. We have analysed the performance of a detector with unprecedented sensitivity, angular and energy resolution and combined with polarimetric capability to study of the most powerful Galactic and extragalactic sources and with a line sensitivity in the MeV energy range two orders of magnitude better than previous generation of instruments that can determine the origin of key isotopes fundamental for the understanding of supernova explosion and the chemical evolution of our Galaxy.

Key words. Gamma Ray– Compton Production– Polarimeter– Silicon Micro-Strip Detector

1. Introduction

e-ASTROGAM (De Angelis et al. 2018) is a gamma-ray space mission that have been proposed as the M5 Medium-size mission of the European Space Agency. It is a gamma-ray instrument that inherits from predecessors such as AGILE (Tavani et al. 2009) and Fermi (Atwood et al. 2009), as well as from the MEGA (Kanbach et al. 2005) prototype and the Gamma-Light project (Morselli et al. 2013) but it takes full advantages of recent progresses in silicon detectors and readout microelectronics to achieve measurement of the energy and 3D position of each interaction within the detectors with an excellent spectral and spatial resolution. The main innovative feature of the e-ASTROGAM mission is the capability of joint detection in the Compton (0.2 - 30 MeV) and pair (>10 MeV) energy ranges in a single integrated instrument. The mission aims at improving the sensitivity in the medium-energy gamma-ray domain by one to two orders of

magnitude compared to previous missions, and it can provide a groundbreaking capability for measuring gamma-ray polarization giving access to a new observable that can provide valuable information on the geometry and emission processes of various high-energy sources.

2. The e-ASTROGAM telescope

The e-ASTROGAM telescope, see Fig. 1, is made up of three detection system: a silicon Tracker in which the cosmic gamma rays undergo a Compton scattering or a pair conversion, a Calorimeter to absorb and measure the energy of the secondary particles, and an anticoincidence (AC) system to veto the prompt-reaction background induced by charged particles. The telescope has a size of $110 \times 110 \times 80$ cm³ and a mass of 820 kg.

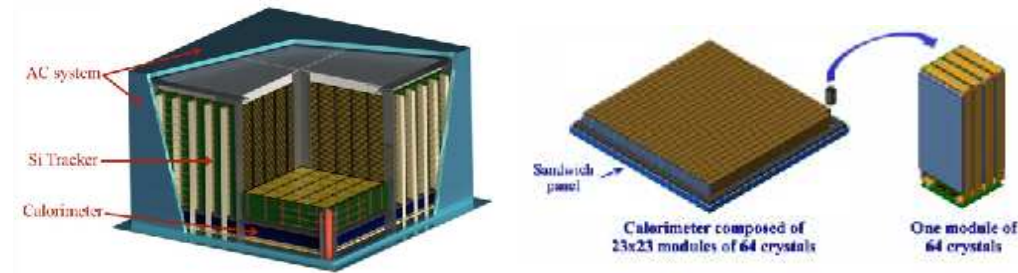


Fig. 1. Overview of the e-ASTROGAM payload showing the silicon Tracker, the Calorimeter and the Anti-coincidence system.

2.1. Silicon Tracker

The e-ASTROGAM Tracker is a double-sided strip detectors (DSSD) that comprises 5600 DSSDs arranged in 56 layers. It is divided in four units of 5×5 DSSDs, the detectors being wire bonded strip to strip to form 2-D ladders. The interlayer distance is 10 mm. Each DSSD has a geometric area of $9.5 \times 9.5 \text{ cm}^2$, a thickness of $500 \mu\text{m}$, and a strip pitch of $240 \mu\text{m}$. The total detection area amounts to 9025 cm^2 and the total Si thickness to 2.8 cm, which corresponds to 0.3 radiation length on axis.

2.2. Calorimeter

The e-ASTROGAM Calorimeter is a pixelated detector made of a high-Z scintillation material, Thallium activated Cesium Iodide. It consists of an array of 33,856 parallelepiped bars of CsI(Tl) of 8 cm length and $5 \times 5 \text{ mm}^2$ cross section, read out by silicon drift detectors (SDDs) at both ends, arranged in an array of 529 ($=23 \times 23$) elementary modules comprising each 64 crystals. The Calorimeter thickness, 8 cm of CsI(Tl), makes it a 4.3 radiation length detector having an absorption probability of a 1-MeV photon on axis of 88%.

2.3. Anticoincidence system

The third main detector of the e-ASTROGAM payload consists of an Anticoincidence (AC) system made of segmented panels of plastic scintillators covering the top and four lateral sides of the instrument, requiring a total active area of about 4.7 m^2 . The AC detector is seg-

mented in 33 plastic tiles (6 tiles per lateral side and 9 tiles for the top). All scintillator tiles are coupled to silicon photomultipliers (SiPM) by optical fibers.

3. Silicon Tracker: Geometry optimization in the Compton regime

We have focus our optimization studies on the silicon tracker geometry. We have perform the simulations, the reconstruction and analysis of the events using the MEGAlib framework (Zoglauer et al. 2006). MEGAlib was develop to simulate tracker detectors in the Compton regime, and recently was update to include also the pair production regime. The detector is simulated using a wrapped of the well know Geant4 framework (Agostinelli et al. 2003). The output of the simulations is reconstructed using the tools *rean* and *mimrec*.

In the energy range from 0.3 to 5 MeV we measured the properties of the incident photon using the Compton effect. From the interaction we have two products, a photon and an electron. If the electron have enough energy will escape the silicon layer and will be detect as it hits other layers. Otherwise we will only have the hits from the photon. We have to distinguish between events with electron tracking and without electron tracking. This will have implications in the angular resolution.

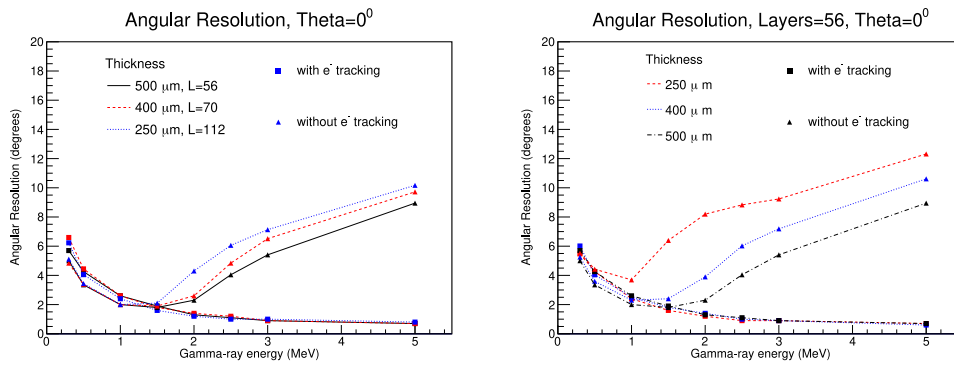


Fig. 2. Angular resolution from the reconstruction of Compton events, Left panel: Fix the radiation length. Right panel: Fix the number of layers.

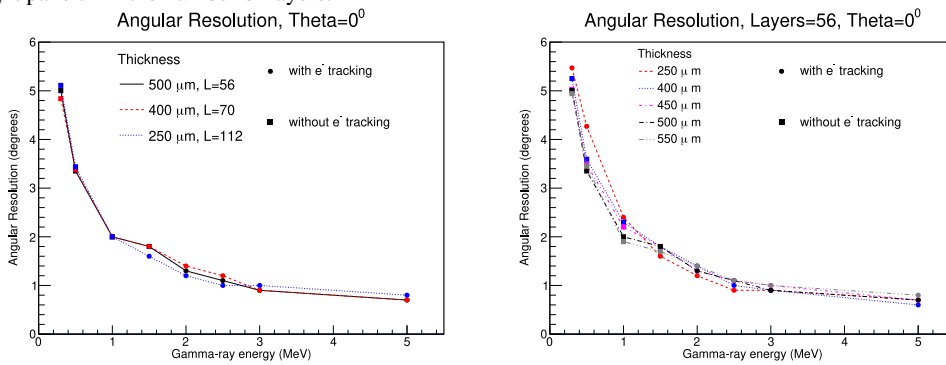


Fig. 3. Angular resolution, after event selection, from the reconstruction of Compton events, Left panel: Fix the radiation length. Right panel: Fix the number of layers.

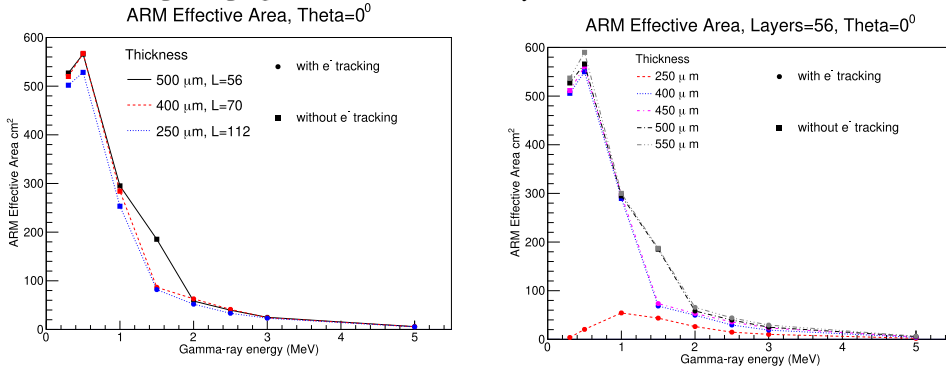


Fig. 4. Effective area from the reconstruction of Compton events, Left panel: Fix the radiation length. Right panel: Fix the number of layers.

3.1. Energy resolution - Photopeak events

In Fig. 3, we show the results of the angular resolution after the event selection. As we can

observe regardless of the geometry we have obtain the same angular resolution within the uncertainties.

The angular resolution goes from 5° at 0.3 MeV to 1° at 5 MeV.

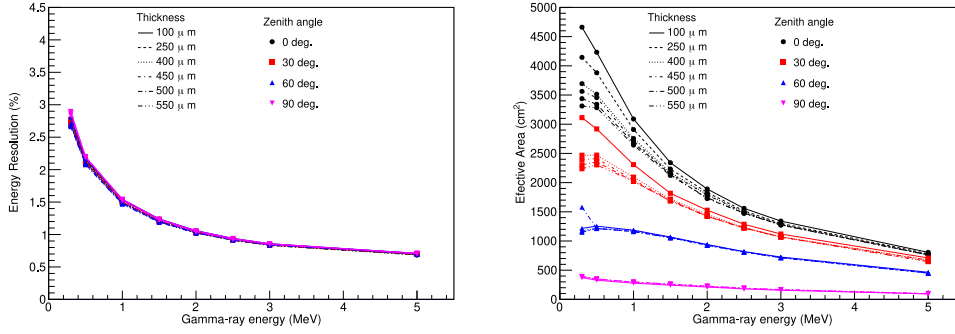


Fig. 5. Energy resolution (left) and Effective area (right) from the photopeak area

We have to use the photopeak events to calculate the energy resolution in the Compton regime. In Fig. 5, we show the results, in the left panel we see that the energy resolution does not depend on any geometrical parameters used in the simulation. We have observed an energy resolution of 3% at low energies that decreases to about 1% at 5 MeV. In the right panel we show the dependence of the effective area as a function of the energy for different thicknesses and zenith angles.

3.2. Angular resolution - Compton events

For the angular resolution we have to take into account the events reconstructed w/o electron tracking. For simplicity we show the results for events simulated with a zenith angle of 0 degrees.

Using the event selection that minimizes the angular resolution we show in Figure 4 the effective area. In the left panel, when the number of total radiation lengths is fixed we have obtained the same effective area independent of the simulated geometry. In the right panel, we have kept the number of layers fixed to 56, in this case we observe that, for low energies, for a thickness of 250 μm the effective area drops dramatically in comparison with 400 and 500 μm.

In Fig. 2 we show, on the left panel, the results for 3 different thicknesses when we have fixed the number of total radiation lengths to $0.3X_0$. For events without electron tracking,

triangles points, we observe that at approximately 1.5 MeV the resolutions start to get worse for all thicknesses. This is not the case for the reconstructed events with electron tracking, square points, the angular resolution gets better as the energy increases, going from $\sim 6^\circ$ at 0.3 MeV to 1° at 5 MeV. For energies below ~ 1.5 MeV both reconstructions give approximately the same angular reconstruction.

In the right panel, we show the results for geometries with different thicknesses but the same number of layers, in this case 56. For events with electron tracking we observe the same results when the total radiation length was fixed. We have found a different situation when we have reconstructed events with no electron tracking. In this case, depending on the thickness, the angular resolutions start getting worse at different energies. We can see that for 250 μm at energies less than 1 MeV the angular resolutions start decreasing, but for 400 and 500 μm this behaviour starts at 1.5 MeV or above.

It is clear that we have to make an event selection to obtain the best angular resolution as a function of the energy and for each simulated geometry.

4. Conclusions

We have simulated different geometries for the eASTROGAM silicon tracker using the MEGALib framework. We have studied the Compton and Pair production regimes by simulating different energies ranging from 0.3 to 5 MeV.

In the Compton regime we have found that the energy resolution does not depend on the simulate geometry.

For the angular resolution we have to make an event selection between reconstructed events w/o electron tracking to obtain the best possible resolution. After the selection the angular resolution is independent of the geometry. We have found difference in the effective area when the number of interactions lengths is smaller than $0.3X_0$, we have observed that, for low energies, for thickness of $250 \mu\text{m}$ the effective area drop dramatically in comparison with 400 and $500 \mu\text{m}$. The similar study in the pair production regime is on-going

Acknowledgements. The research leading to these results has received funding from the European Union's Horizon 2020 Programme under the AHEAD project (grant agreement n. 654215)

References

- Agostinelli, S., et al. 2003, Nuclear Instruments and Methods in Physics Research A, 506, 250
- Atwood, W. B., Abdo, A. A., Ackermann, M., et al. 2009, ApJ, 697, 1071
- de Angelis, A., Tatischeff, V., Grenier, I. A., et al. 2018, Journal of High Energy Astrophysics, 19, 1
- Kanbach, G., Andritschke, R., Zoglauer, A., et al. 2005, Nuclear Instruments and Methods in Physics Research A, 541, 310
- Morselli, A., Argan, A., Barbiellini, G., et al. 2013, Nuclear Physics B Proceedings Supplements, 239, 193
- Tavani, M., Barbiellini, G., Argan, A., et al. 2009, A&A, 502, 995
- Zoglauer, A., et al. 2006, New Astronomy Reviews, 50, 7